JOURNAL OF MATERIALS SCIENCE 29 (1994) 5115–5120

Synthesis of $PbTiO_3$ film on $LaNiO_3$-coated substrate by the spray–ICP technique

H. ICHINOSE, M. NAGANO
Department of Applied Chemistry, Saga University, 1, Honjou-machi, Saga-shi 840, Japan
H. KATSUKI, H. TAKAGI
Saga Ceramics Research Laboratory, 3100-5, Arita-machi, Nishimatsuura-gun, Saga 844, Japan

In an attempt to utilize $LaNiO_3$ as a bottom electrode for $PbTiO_3$ ferroelectric film, $PbTiO_3$ and $LaNiO_3$ films were prepared by the spray–ICP technique under atmospheric pressure. The dense $LaNiO_3$ films crystallized with preferred (1 1 1) and (1 0 0) orientations on sapphire (0 0 1) and MgO (1 0 0), respectively. Resistivities of the $LaNiO_3$ films deposited above 600 °C were about $4 \times 10^{-6}\ \Omega$ m. The $PbTiO_3$ film with preferred (0 0 1) orientation was successfully prepared on $LaNiO_3$-coated MgO (1 0 0). Its dielectric constant and dissipation factor were about 200 and 0.02, respectively, at 1 kHz. The Curie temperature suggested that $PbTiO_3$ films were free from contamination by $LaNiO_3$.

1. Introduction

Thin $PbTiO_3$ films are well known as useful ferroelectrics [1, 2] and have received considerable attention for microelectronic applications. Thin $PbTiO_3$ films have been widely prepared by r.f. sputtering [3, 4], chemical vapour deposition [5, 6], laser ablation [7] and the sol–gel method [8]. The pyroelectric property of $PbTiO_3$ requires (0 0 1) orientation because of the polarization axis parallel to ⟨0 0 1⟩. Although noble metals such as platinum or palladium have been used as the electrodes for $PbTiO_3$ capacitors, there are some problems; expensiveness, weak adhesion to the substrate [4] and contamination by the interdiffusion from the substrates [9]. On the other hand, $LaNiO_3$ has a perovskite structure similar to $PbTiO_3$ and shows a metallic conductivity. $LaNiO_3$ film is, therefore, expected to be the favoured bottom electrode for $PbTiO_3$ dielectric film. The rhombohedral perovskite of $LaNiO_3$ has been favoured for electrodes [10], electrocatalysts and alcohol sensors [11, 12]. However, preparation of dense single-phase $LaNiO_3$ is difficult by a conventional sintering method, owing to the ease of decomposition to $La_2NiO_4 + La_2O_3 + NiO$ above 1120 °C [13]. Therefore, Na_2CO_3 flux as a sintering aid [14] or a precursor such as acetate [13] has been used in the preparation of $LaNiO_3$, or high-pressure techniques such as hot pressing (HP) [15] or hot isostatic pressing (HIP) [16] have been employed.

The spray pyrolysis technique, assisted by an inductively coupled plasma (spray–ICP technique) has many advantages; it is free from contamination by the electrode, unstable phase formation or fast deposition rate due to the ultra-high temperature reaction, and easy composition control using aqueous source solutions [17–21]. Oriented $PbTiO_3$ films were recently prepared on sapphire (0 0 1) and MgO (1 0 0) substrates by this method [22]. However, in order to utilize $PbTiO_3$ films in microelectronic fields, it is necessary to prepare (0 0 1)-oriented $PbTiO_3$ films on electrically conductive films for use as the bottom electrode. This study was focused on the preparation of a conductive $LaNiO_3$ film as a new bottom electrode by the spray–ICP technique and the formation of (0 0 1)-oriented $PbTiO_3$ films on the $LaNiO_3$-coated substrates.

2. Experimental procedure

Mother solutions were prepared by dissolving $La(NO_3)_3 \cdot 6\,H_2O$, $Ni(NO_3)_2 \cdot 6\,H_2O$, $Pb(NO_3)_2$ or $TiO(NO_3)_2$ in distilled water in the required stoichiometric ratio (La:Ni or Pb:Ti = 1:1, total concentration of metal = 0.25 M). The spray–ICP technique employed here was similar to that originally reported by Kagawa *et al.* [20], and used previously to prepare oriented films of $PbTiO_3$ on various substrates [22]. The spray–ICP technique was described in detail in the previous paper [22]. Typical conditions of the spray–ICP technique in this study are shown in Table I. Sintered high-purity alumina, Si (1 0 0), sapphire (0 0 1) and MgO (1 0 0) plates (10–20 mm wide by 0.5 mm thick) were used as substrates. The substrate was heated to 350–800 °C by the ICP flame.

The films were investigated by X-ray diffraction (XRD), scanning electron microscopy (SEM) and X-ray microprobe analysis (XMPA). The film compositions were determined by an ICP spectroscopic analysis after the films were dissolved in concentrated nitric acid. Electrical resistivities of $LaNiO_3$ films were

0022–2461

TABLE I Typical spray–ICP conditions for deposition

R.f. frequency	4 MHz
R.f. power	6–7 kW
Pressure	760 torr
Plasma gas (Ar)	15 SLM
Sheath gas (Ar)	10 SLM
(O_2)	2 SLM
Carrier gas (Ar)	2 SLM
Position of substrate from centre of work coil	35 mm
Feed rate of mother solution	20 ml h^{-1}

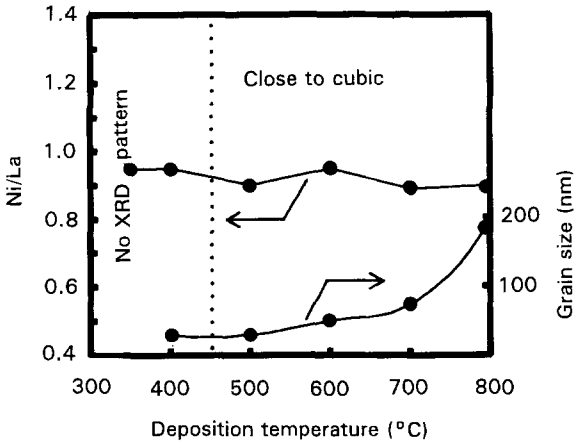

Figure 1 The effect of deposition temperature on composition and grain size of $LaNiO_3$ film deposited on sintered alumina.

measured by the standard four-probe technique using sputtered gold as the electrodes. Capacitors were formed by sandwiching a $PbTiO_3$ film between a bottom electrode ($LaNiO_3$ film) and a top electrode (sputtered gold). The dielectric properties were measured by using a LCZ meter (2330, NF Electronic Instruments).

3. Results and discussion

3.1. Properties of $LaNiO_3$ films

Fig. 1 shows the effect of substrate temperature on the composition and grain size of $LaNiO_3$ films deposited on sintered alumina substrates. The atomic ratios Ni/La of the films were 0.9–0.95 and equal to that of the mother solution. The splitting of (1 1 0) and (1 0 1) diffraction peaks was not so clear in XRD patterns of $LaNiO_3$ films obtained at 500–800 °C that the crystallographic structure of the films were presumed to be still rhombohedral (low-temperature phase), but it was close to the cubic form (high-temperature phase) [13]. Obayashi and Kudo [13] reported that the rhombohedral–cubic transition was observed at 940 °C. The reasons why the structure of $LaNiO_3$ film was close to the high-temperature phase, in spite of a lower deposition temperature than the transition temperature, may be as follows: (1) the very small grain size of $LaNiO_3$ (< 100 nm) caused the appearance of the high-temperature phase, as shown in the case of $PbTiO_3$ [23]; (2) the highly activated species in the high-temperature ICP formed the high-temperature phase of $LaNiO_3$ which was quenched.

Fig. 2 shows the electrical resistivity of $LaNiO_3$ films deposited on an alumina substrate. The electrical resistivity decreased with increasing deposition temperature, and low resistivities of about 4×10^{-6} Ω m were obtained for the films deposited above 600 °C. Because the reported electrical conductivity of dense $LaNiO_3$ prepared by HIP at 1400 °C was 2.2×10^{-6} Ω m [16], $LaNiO_3$ films obtained above 600 °C in this study were deduced to be fairly dense.

Fig. 3 shows XRD patterns of films deposited at 800 °C on the substrates of sintered alumina, Si (1 0 0), sapphire (0 0 1) and MgO (1 0 0). The $LaNiO_3$ films crystallized with preferred (1 1 0), (1 0 $\bar{1}$), (1 1 1) and (1 0 0) orientations on sintered alumina, Si (1 0 0), sapphire (0 0 1) and MgO (1 0 0), respectively. In particular, the $LaNiO_3$ film on MgO (1 0 0) oriented preferentially: it was found on the various substrates of single crystal as well as on the polycrystalline substrate of sintered alumina that $LaNiO_3$ films crystallized in a form close to the high-temperature phase (cubic). SEM images of $LaNiO_3$ films deposited on sintered alumina, Si (1 0 0), sapphire (0 0 1) and MgO (1 0 0) at 800 °C are compared in Fig. 4. The microstructures of these films depended significantly on the substrates. The films on sintered alumina and Si (1 0 0) were composed of particles 0.1–0.2 μm in size. On sapphire, a smooth surface consisted of particles with triangular planes parallel to the substrate, suggesting the (1 1 1) orientation of the particles. The film on MgO was also very smooth and dense. Several rod-like particles were observed on the surface. The textures of the smooth surfaces and the arrangements of the particles on sapphire and MgO suggested an expitaxial growth. Confirmation was left for future experiments.

3.2. $PbTiO_3$ films deposited on the $LaNiO_3$ films

In order to use $LaNiO_3$ as a bottom electrode for

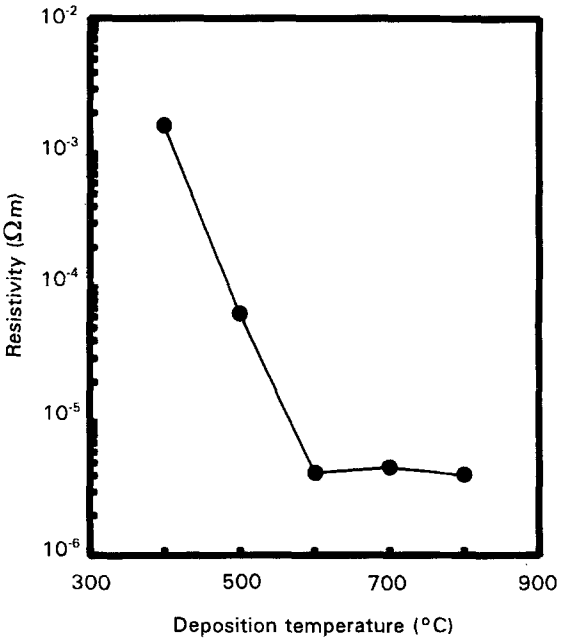

Figure 2 The effect of deposition temperature on resistivity of $LaNiO_3$ film deposited on sintered alumina.

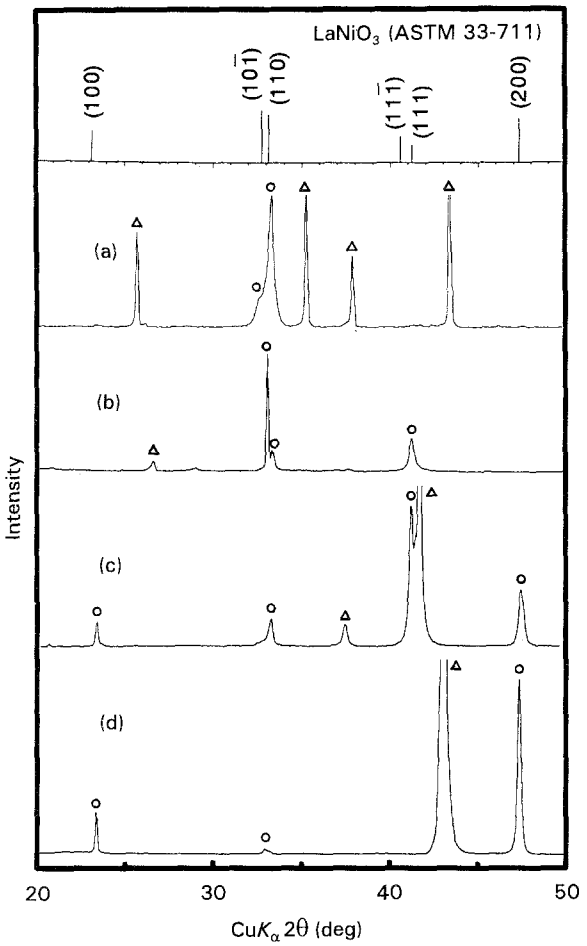

Figure 3 XRD patterns of $LaNiO_3$ films deposited at 800 °C on (a) sintered alumina, (b) Si (1 0 0), (c) sapphire (0 0 1) and (d) MgO (1 0 0). (○) $LaNiO_3$, (△) substrate.

$PbTiO_3$ dielectric film, $PbTiO_3$ films were formed on $LaNiO_3$-coated substrates. Fig. 5 shows XRD patterns of $PbTiO_3$ films deposited on $LaNiO_3$-coated various substrates. The substrate temperatures were kept at 800 and 650 °C during deposition of $LaNiO_3$ and $PbTiO_3$, respectively. The film of $PbTiO_3$ deposited on sintered alumina coated with $LaNiO_3$ was not oriented. The $PbTiO_3$ films on silicon, sapphire and MgO crystallized preferentially with (1 1 1), (1 1 1) and (0 0 1) orientations. The degree of c-axis orientation, $\alpha = \Sigma I(0\,0\,1)/\Sigma I(h\,k\,l)$, of the film deposited on MgO was 0.8–0.9, where $I(0\,0\,1)$ and $I(h\,k\,l)$ are the XRD intensities of (0 0 1) and $(h\,k\,l)$ reflections. This value was equivalent to that obtained by a sputtering method [24]. It should be noted that (1 1 1) orientation appeared on $LaNiO_3$-coated silicon substrate, whereas orientation of the film was not observed on silicon without an $LaNiO_3$-coating [22]. The preferred orientation on $LaNiO_3$-coated silicon may be attributed to the oriented $LaNiO_3$ film which has a similar perovskite-type structure to $PbTiO_3$.

Fig. 6 shows SEM images of cross-sections of these films. $PbTiO_3$ particles on $LaNiO_3$-coated sapphire and silicon were columnar. Their coagulation was not so tight. On the other hand, films on $LaNiO_3$-coated sintered alumina and especially on $LaNiO_3$-coated MgO, were densely coagulated. It should be noted that the film on $LaNiO_3$-coated MgO had a smoother surface than that deposited directly onto MgO without an $LaNiO_3$-coating [22]. The $PbTiO_3$ particles on this smooth film had a square plane, and the edges were parallel to the ⟨0 0 1⟩ direction of the MgO substrate, as shown in Fig. 7. An epitaxial growth of $PbTiO_3$ on $LaNiO_3$-coated MgO is suggested.

3.3. Dielectric properties

When the $LaNiO_3$ film is utilized as a bottom electrode for $PbTiO_3$ ferroelectric film, there is the risk of contamination by diffusion of $LaNiO_3$ to the $PbTiO_3$ layer during deposition. The contamination with lanthanum in the $PbTiO_3$ film may cause the formation of $Pb_{1-x}La_{2x/3}TiO_2$ and result in a lowering of the Curie temperature. In order to confirm this point, the temperature dependence of dielectric constants, (ε_r), was investigated for the dense $PbTiO_3$ films obtained on $LaNiO_3$-coated MgO and sintered alumina (thickness about 0.5 μm). The results are shown in Fig. 8. The maximum dielectric constant due to the ferroelectric–paraelectric phase transition was clearly observed at about 490 °C for both films, and the relationship between ε_r and T followed the Curie–Weiss law above 490 °C. This transition temperature agreed closely with that of pure $PbTiO_3$ ceramics. This result suggested that the contamination with $LaNiO_3$ in the $PbTiO_3$ layer was negligible, and that the $LaNiO_3$ interlayer was a good bottom electrode for $PbTiO_3$ dielectric film.

Table II shows the ε_r and the dissipation factor, tan δ, measured at 1 kHz and at room temperature. ε_r of $PbTiO_3$ films deposited at 650 °C on $LaNiO_3$-coated MgO and sintered alumina were 197 and 125, respectively, for a film thickness of about 0.6 μm. This difference was deduced to be attributed to the difference in the densities of films. ε_r decreased for the films deposited on $LaNiO_3$-coated MgO at 600 and 700 °C. The lower ε_r might be attributed to the thinness of the film (about 0.4 μm) [3]. Tan δ had the relatively small value of 0.017–0.08.

TABLE II ε_r and tan δ of $PbTiO_3$ film measured at 1 kHz

Sample	Substrate	Deposition temp. (°C)	Thickness (μm)	ε_r	Tan δ
1	$LaNiO_3/Al_2O_3$	650	0.6	125	0.08
2	$LaNiO_3$/MgO(1 0 0)	600	0.44	101	0.03
3	$LaNiO_3$/MgO(1 0 0)	650	0.63	197	0.08
4	$LaNiO_3$/MgO(1 0 0)	700	0.43	144	0.017

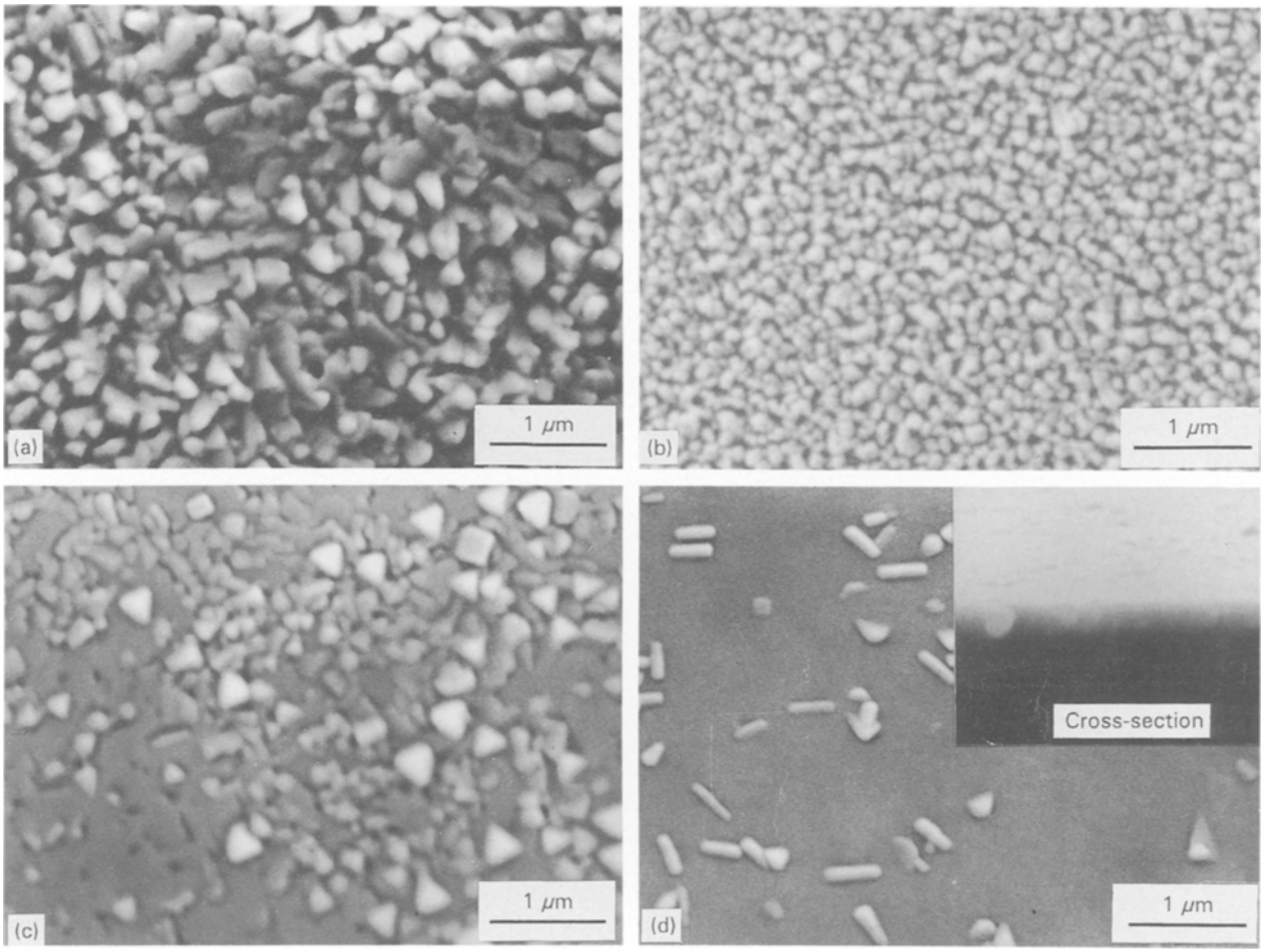

Figure 4 SEM images of $LaNiO_3$ films deposited at 800 °C on (a) sintered alumina, (b) Si (1 0 0), (c) sapphire (0 0 1) and (d) MgO (1 0 0). The insert in (d) is a surface observed from the film edge.

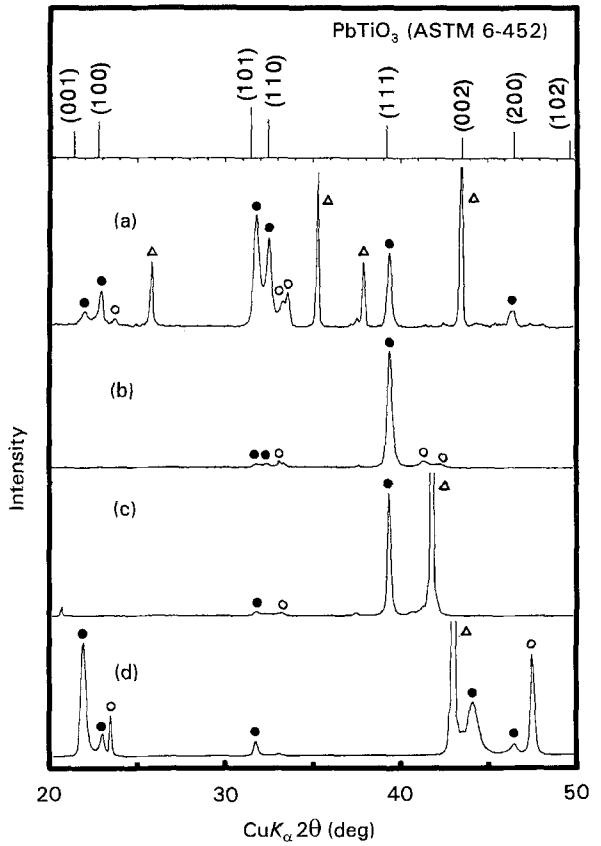

Figure 5 XRD patterns of $PbTiO_3$ films deposited at 650 °C on $LaNiO_3$-coated substrates: (a) sintered alumina, (b) Si (1 0 0), (c) sapphire (0 0 1) and (d) MgO (1 0 0). (○) $LaNiO_3$, (●) $PbTiO_3$, (△) substrate.

4. Conclusion

In order to utilize $LaNiO_3$ as a bottom electrode for $PbTiO_3$ ferroelectric film, $PbTiO_3$ was deposited on $LaNiO_3$-coated substrate by the spray–ICP technique. Single phases of perovskite-type $LaNiO_3$ and $PbTiO_3$ were obtained at 500–800 °C. Most of the films had relatively dense structures. In particular, $PbTiO_3$ obtained on $LaNiO_3$-coated MgO (1 0 0) was denser than that deposited directly on MgO (1 0 0). Because this film crystallized with the (0 0 1) orientation perpendicular to the polarization axis, the dielectric constant was relatively high (about 200 at 1 kHz). It should be noted that excellent films could be obtained by the spray–ICP process, as quickly by the MOCVD method, but which requires a reduced atmosphere and expensive source materials. These preferentially oriented films were attributed to the successful preparation of dense, oriented $LaNiO_3$ film, which had the same type of crystal structure as $PbTiO_3$ and a high electrical conductivity. In addition, the contamination of $PbTiO_3$ films from the $LaNiO_3$ layer was found to be negligible. It was, therefore, believed that the $LaNiO_3$ film was a more favourable electrode for $PbTiO_3$ dielectric film than the conventional platinum electrode. Other lanthanum series perovskites could also be expected to be used as electrodes for dielectric films.

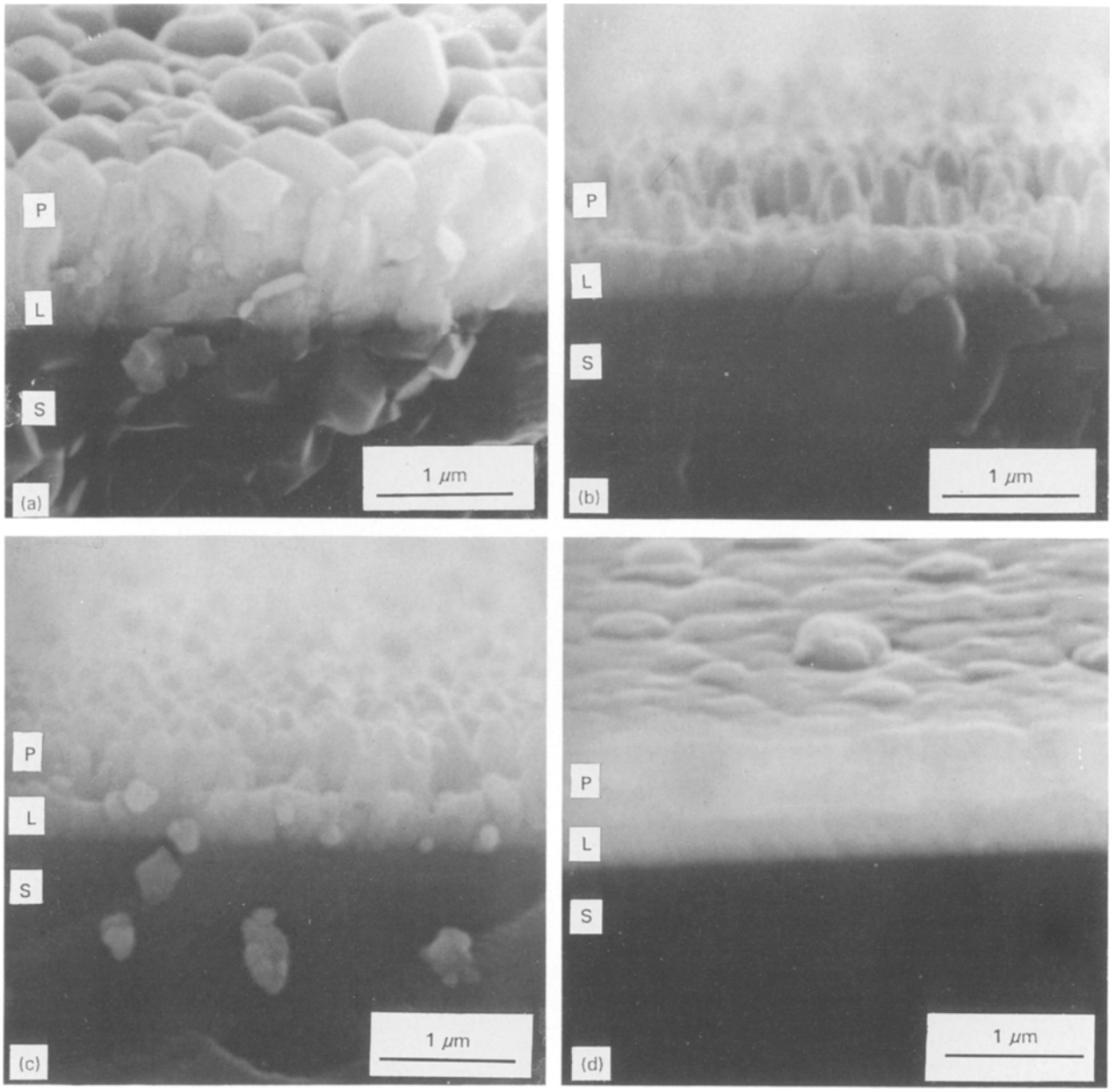

Figure 6 Cross-sections of $PbTiO_3/LaNiO_3$ films deposited on (a) sintered alumina, (b) Si (1 0 0), (c) sapphire (0 0 1) and (d) MgO (1 0 0). P, L and S refer to layer of $PbTiO_3$, $LaNiO_3$ and substrate, respectively.

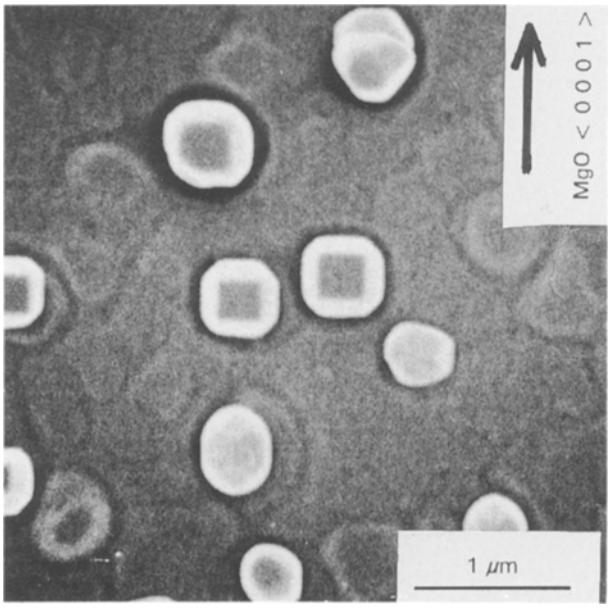

Figure 7 $PbTiO_3$ particles deposited on $PbTiO_3$ film which was prepared on $LaNiO_3$-coated MgO (1 0 0).

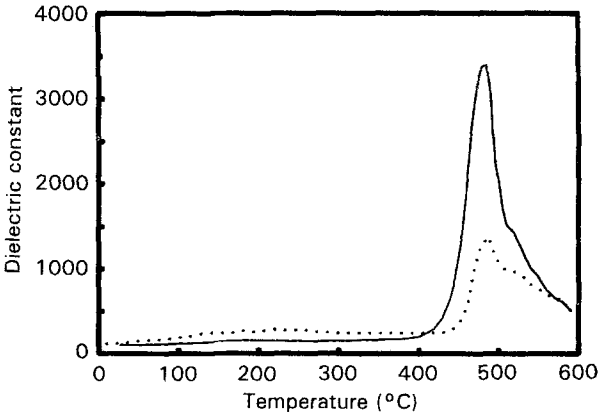

Figure 8 Temperature dependence of dielectric constant of $PbTiO_3$ film deposited on $LaNiO_3$-coated substrate (at 1 kHz). (——) $PbTiO_3/LaNiO_3/MgO$, 600 °C; (···) $PbTiO_3/LaNiO_3/Al_2O_3$, 650 °C.

Acknowledgements

The authors thank Dr M. Kagawa, Institute for Materials Research, Tohoku University, for useful suggestions.

References

1. G. SHIRANE, R. PEPINSKY and B. C. FRAZER, *Acta. Crystallogr.* **9** (1956) 131.
2. V. G. BHIDE, M. S. HEGDE and K. G. DESHMUKH, *J. Am. Ceram. Soc.* **51** (1968) 565.
3. M. OKUYAMA, Y. MATSUI, H. NAKANO, T. NAKAGAWA and Y. HAMAKAWA, *Jpn J. Appl. Phys.* **18** (1979) 1633.
4. K. ABE, H. TOMITA, H. TOYOTA, M. IMAI and Y. YOKOTE, *ibid.* **30** (1991) 2152–54.
5. T. NAKAGAWA, J. KAWAGUCHI, M. OKUYAMA and Y. HAMAKAWA, *ibid.* **21** (1982) L655.
6. A. ANDO, T. KATAYAMA, M. SHIMIZU and T. SHIOSAKI, *ibid.* **31** (1992) 3001.
7. H. TABATA, O. MURATA, T. KAWAI, S. KAWAI and M. OKUYAMA, *ibid.* **31** (1992) 2968.
8. S. L. SWARTZ, S. J. BRIGHT, P. J. MELLING and T. R. SHROUT, *Ferroelectrics* **108** (1990) 71.
9. S. MATSUBARA, T. SAKUMA, S. YAMAMICHI, H. YAMAGUCHI and Y. MIYASAKA, *Mater. Res. Soc. Symp. Proc.* **200** (1990) 243.
10. Y. MATSUMOTO, H. YONEYAMA and H. TAMURA, *Chem. Lett.* (1975) 661.
11. Y. MATSUMOTO, S. YAMADA, T. NISHIDA and E. SATO, *J. Electrochem. Soc.* **127** (1980) 2360.
12. H. OBAYASHI, Y. SAKURAI and T. GETO, *J. Solid State Chem.* **17** (1976) 299.
13. H. OBAYASHI and T. KUDO, *Jpn J. Appl. Phys.* **14** (1975) 330.
14. A. WOLD, B. POST and E. BANKS, *J. Am. Chem. Soc.* **79** (1957) 4911.
15. M. C. KIM, S. J. PARK, H. HANEDA, A. WATANABE, J. TANAKA and S. SHIRASAKI, *Jpn J. Ceram. Soc.* **97** (1989) 1129.
16. K. KAMATA, S. OHSHIO, K. TNAKA, K. KAWAI, T. YMADA and J. NISHINO, *Jpn J. Ceram. Soc.* **100** (1992) 972 (in Japanese).
17. M. KAGAWA, M. KIKUCHI, R. OHNO and T. NAGAE, *J. Am. Ceram. Soc.* **64** (1981) C7.
18. M. KAGAWA, M. KIKUCHI, Y. SYONO and T. NAGAE, *ibid.* **66** (1983) 751.
19. T. ONO, M. KAGAWA and Y. SHONO, *J. Mater. Sci.* **20** (1985) 2483.
20. M. KAGAWA, H. KOMATSU, Y. SYONO and A. YAMADA, *Adv. Ceram.* **24** (1988) 951.
21. M. SUZUKI, M. KAGAWA, Y. SYONO and T. HIRAI, *J. Crystal Growth* **99** (1990) 611.
22. H. ICHINOSE, H. KATSUKI, H. TAKAGI and M. NAGANO, *J. Mater. Sci.* **29** (1994).
23. K. UCHINO, E. SADANAGA and T. HIROSE, *J. Am. Ceram. Soc.* **72** (1989) 1555.
24. K. IIJIMA, Y. TOMITA, R. TAKAYAMA and I. UEDA, *J. Appl. Phys.* **60** (1986) 361.

Received 11 June 1993
and accepted 19 January 1994